AEM JOURNAL.ORG

Multi-Objective Optimization-Based Operational Strategy for Highway Service Area Integrated Energy Systems

Yongjun Zhou[1], Menghao Duan[1], Junzu Liu[1], Haipin Huang[1]
[1]Gezhouba (Wuhan) New Energy Technology Development Co., Ltd., Wuhan 430033, Hubei, China
Corresponding author: Haipin Huang (e-mail: 18573140617@163.com)

ABSTRACT Highway service area integrated energy systems are facing increasing operational challenges caused by the rapid growth of electric vehicle charging demand, renewable energy uncertainty, and low-carbon operation requirements. To address these challenges, this study proposes a multi-objective optimization framework for HSA-IES operation considering operational cost, carbon emissions, and renewable energy utilization. The proposed system integrates photovoltaic generation, combined heat and power units, battery energy storage, flexible electric vehicle charging, heating and cooling subsystems, and grid interaction. A multi-energy coupling model is established, and an enhanced NSGA-II algorithm is adopted to obtain Pareto-optimal scheduling solutions under stochastic renewable generation and traffic-induced load fluctuations. Simulation results show that the proposed strategy reduces operational cost by approximately 12.7% and carbon emissions by approximately 18.2% compared with a conventional rule-based strategy, while renewable energy utilization increases from 72.6%±2.4% to 86.1%±2.3%. From an advanced engineering perspective, the system involves power-electromagnetic coupling, grid-connected conversion, EV charging interfaces, and intelligent energy-management communication. The results provide decision support for low-carbon and robust highway energy operation.

INDEX TERMS highway service area,integrated energy system,multi-objective optimization,electric vehicle charging,powerelectromagnetic coupling

I. INTRODUCTION

WITH the continuous expansion of highway transportation networks and the rapid growth of traffic flow, highway service areas (HSAs) have become important infrastructures for providing energy supply and public services to travelers. Modern HSAs consume considerable amounts of electricity, heating, and cooling energy due to the increasing operation of lighting systems, ventilation equipment, commercial facilities, and electric vehicle (EV) charging stations. Conventional energy supply modes, which mainly rely on grid electricity and fossil-fuel-based thermal systems, often suffer from low energy utilization efficiency, high operational cost, and significant carbon emissions. Therefore, improving the operational efficiency and sustainability of HSA energy systems has become an important research topic in the context of low-carbon energy transition and intelligent transportation development.

Integrated energy systems (IESs), which coordinate multiple energy carriers such as electricity, heating, cooling, and natural gas, provide an effective solution for enhancing energy utilization efficiency and renewable energy accommodation [1-3]. Through the coordinated operation of distributed generation units, energy storage systems (ESSs), and multi-energy conversion devices, IESs can significantly improve system flexibility and operational economic efficiency. Energy hub theory and multi-energy flow modeling have been widely adopted to characterize the coupling relationships among different energy subsystems [3]. Meanwhile, renewable energy technologies such as photovoltaic (PV) generation and distributed wind power have been increasingly integrated into IESs to reduce dependence on conventional fossil fuels and mitigate greenhouse gas emissions.

To optimize the operation of integrated energy systems, various intelligent optimization algorithms have been developed in recent years. Particle swarm optimization (PSO) has demonstrated good convergence characteristics and computational efficiency in complex energy scheduling problems [4]. In addition, multiobjective evolutionary algorithms such as the Non-dominated Sorting Genetic Algorithm II (NSGA-II) and Multi-Objective Evolutionary Algorithm Based on Decomposition (MOEA/D) have been extensively applied to address the trade-off relationships among operational cost, energy efficiency, and environmental impact [5-7]. Compared with conventional single-objective optimization approaches, multi-objective optimization methods can provide a set of Pareto-optimal solutions, enabling decision-makers to select appropriate operational strategies according to different practical requirements.

Existing studies have investigated integrated energy dispatch, combined heat and power (CHP) flexibility enhancement, integrated demand response, and energy hub operational optimization [8]. CHP flexibility has been analyzed for renewable energy integration [8], while integrated demand response technologies have been reviewed in multi-energy systems [9]. Optimal operational strategies for combined cooling, heating, and power (CCHP) systems under different operating modes have also been proposed [10]. In addition, integrated energy system operation considering energy trading mechanisms and demand-side management has been further explored [11]. Energy hub-based operational modeling and planning strategies have also been extensively investigated to improve multi-energy coordination and system efficiency [12-14].

However, studies specifically focusing on highway service area integrated energy systems remain relatively limited. HSAs exhibit unique operational characteristics, including highly time-varying traffic-related loads, uncertain EV charging demand, and strong fluctuations in renewable energy generation. Moreover, the operational scheduling of HSA energy systems must simultaneously consider economic performance, renewable energy utilization, system reliability, and environmental impact. The intermittency of renewable energy generation further introduces uncertainty into system operation, thereby requiring robust and flexible energy management strategies [15,16]. Meanwhile, the integration of energy storage technologies has become increasingly important for improving renewable energy accommodation and enhancing operational reliability [17,18].

To address the above challenges, this study proposes a multi-objective optimization strategy for the operation of highway service area integrated energy systems. The proposed framework simultaneously considers operational cost, renewable energy utilization, and carbon emissions while incorporating renewable energy generation, ESSs, and integrated demand response. A detailed HSA integrated energy system model is established, including electricity, heating, cooling, and EV charging subsystems. NSGA-II is employed to obtain Pareto-optimal operational solutions under different operating scenarios. In addition, sensitivity analyses are conducted to evaluate the effects of renewable energy fluctuations and ESS capacity variation on system performance.

The main contributions of this study are summarized as follows: Unlike standard energy hubs, this study develops a refined HSA-IES model that incorporates a dynamic multi-agent reinforcement constraints for EV charging and an enhanced NSGA-II variant. The innovation lies in the integration of band-limited stochastic disturbance signals directly into the genetic operations, improving the scheduling robustness against non- Gaussian traffic-induced load volatility. A multi-objective operational optimization framework is proposed to simultaneously minimize operational cost and carbon emissions while improving renewable energy utilization efficiency. The effectiveness and robustness of the proposed strategy are validated through simulation studies under multiple operating conditions, providing practical references for the sustainable operation of highway service areas.

II. HIGHWAY SERVICE AREA INTEGRATED ENERGY SYSTEM MODELING

A. SYSTEM CONFIGURATION

The integrated energy system (IES) of a highway service area (HSA) consists of multiple energy generation, conversion, storage, and consumption units, enabling the coordinated management of electricity, heating, and cooling energy [1-3]. The proposed system mainly includes photovoltaic (PV) generation units, energy storage systems (ESSs), combined heat and power (CHP) units, electric chillers, gas boilers, electric vehicle (EV) charging stations, and grid interaction modules. Through the coordinated operation of these subsystems, the IES can improve energy utilization efficiency, reduce dependence on conventional fossil-fuel energy, and enhance operational flexibility [2,3].

Figure 1 illustrates the overall structure and energy flow relationships of the proposed HSA integrated energy system. The PV subsystem converts solar energy into electricity to support local electrical loads and reduce grid electricity purchase. The CHP unit simultaneously generates electricity and thermal energy from natural gas, thereby improving primary energy utilization efficiency [8,10]. The thermal energy produced by the CHP unit can be directly supplied to thermal loads and cooling-related energy demand. Meanwhile, the ESS is used to smooth renewable energy fluctuations and support peak-shaving and valley-filling operations. The overall system architecture is shown in Figure 1.

The electrical loads mainly include lighting systems, ventilation equipment, commercial facilities, EV charging stations, and auxiliary service equipment. Thermal and cooling loads are associated with indoor heating, air-conditioning systems, and hot water supply. Since the operating conditions of HSAs vary significantly with traffic flow and seasonal climate conditions, the integrated energy system must have sufficient operational flexibility and energy management capability.

B. LOAD MODELING

The load characteristics of HSAs exhibit significant temporal variability due to changes in traffic volume, ambient temperature, and user activities. Such variability is similar to the dynamic load behavior observed in integrated energy systems and microgrids [9,15]. In this study, the total electrical load is divided into conventional service-area load and EV charging load. Conventional electrical loads mainly include lighting, ventilation, office facilities, and commercial electricity consumption, while EV charging

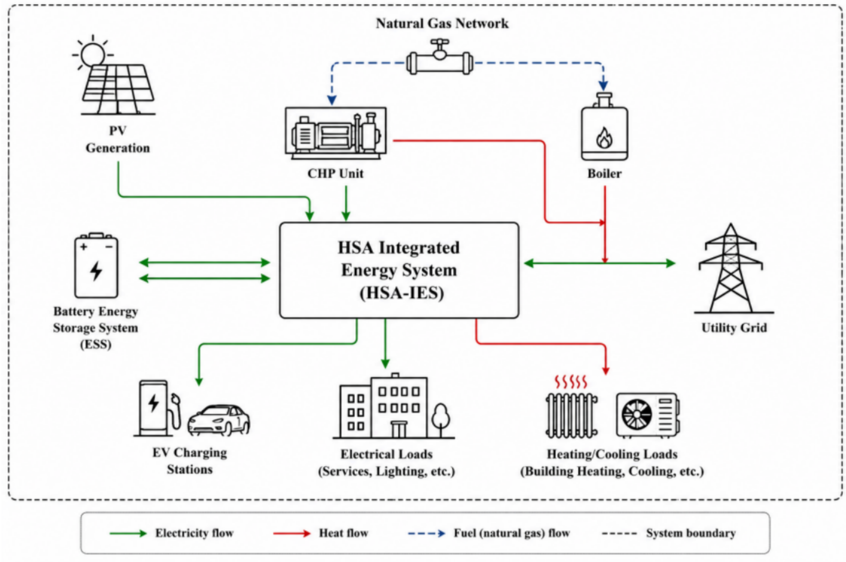

FIGURE 1. Structure and energy flow relationships of the proposed highway service area integrated energy system (HSA-IES)

demand is strongly affected by traffic flow and charging behavior.

The electrical load at time t can be expressed as:

$$P_{\text{load}}(t) = P_{\text{base}}(t) + P_{\text{EV}}(t) \tag{1}$$

where $P_{\text{base}}(t)$ denotes the conventional electrical load, and $P_{\text{EV}}(t)$ represents EV charging demand. Thermal load mainly consists of heating and hot water demand, while cooling load is associated with air-conditioning systems. To reflect realistic operational conditions, load fluctuations are modeled using stochastic variations of approximately $\pm 10\%$–25% based on historical traffic and weather data. This range accounts for standard daily variations as well as significant traffic surges during holiday periods, ensuring the model's validity under extreme peak loads. The daily load profile generally exhibits peak demand during daytime and holiday travel periods, whereas nighttime demand remains relatively low. These dynamic load characteristics require the energy management system to continuously adjust operational strategies according to varying demand conditions.

C. PHOTOVOLTAIC GENERATION MODELING

Photovoltaic generation is one of the primary renewable energy sources integrated into the HSA energy system and has been widely adopted in modern multi-energy systems [8,15]. The output power of the PV system mainly depends on solar irradiance and module conversion efficiency. The PV output power at time t can be calculated as:

$$P_{\text{PV}}(t) = \eta_{\text{PV}} A_{\text{PV}} G(t) \tag{2}$$

where η_{PV} is the photovoltaic conversion efficiency, A_{PV} is the effective panel area, and $G(t)$ denotes solar irradiance at time t.

Considering the intermittency and uncertainty of solar energy, PV output is modeled with time-varying fluctuations. Weather-related uncertainties are introduced through stochastic disturbance terms to improve the realism of the simulation model.

D. ENERGY STORAGE SYSTEM MODELING

The ESS plays an important role in balancing power supply and demand, enhancing renewable energy accommodation, and improving system operational reliability [15-18]. In this study, battery energy storage is adopted to perform energy shifting and peak-load regulation.

The state of charge (SOC) of the ESS is updated according to the following equation:

$$SOC(t+1) = SOC(t) + \frac{\eta_{\text{ch}} P_{\text{ch}}(t)\Delta t}{E_{\max}} - \frac{P_{\text{dis}}(t)\Delta t}{\eta_{\text{dis}} E_{\max}} \tag{3}$$

where $SOC(t)$ is the battery state of charge, $P_{\text{ch}}(t)$ and $P_{\text{dis}}(t)$ denote the charging and discharging power, η_{ch} and η_{dis} represent the charging and discharging efficiencies, $E_{\max}$ is the maximum storage capacity, and Δt is the scheduling interval.

The ESS model and operational constraints are established according to typical battery scheduling approaches reported in previous studies [17,18]. To ensure safe operation, the ESS is constrained by SOC limits:

$$SOC_{\min} \le SOC(t) \le SOC_{\max} \tag{4}$$

Additionally, charging and discharging power must satisfy equipment operational constraints.

E. COMBINED HEAT AND POWER SYSTEM MODELING

The CHP unit simultaneously generates electricity and thermal energy through natural gas consumption, thereby improving overall energy utilization efficiency [8,10]. The electrical and thermal outputs of the CHP unit can be expressed as:

$$\begin{aligned} P_{\text{CHP}}(t) &= \eta_e F_{\text{gas}}(t), \\ Q_{\text{CHP}}(t) &= \eta_h F_{\text{gas}}(t) \end{aligned} \tag{5}$$

where $F_{\text{gas}}(t)$ denotes natural gas consumption, and η_e and η_h are the electrical and thermal conversion efficiencies, respectively.

The CHP unit operates within minimum and maximum output limits:

$$P_{\text{CHP}}^{\min} \leq P_{\text{CHP}}(t) \leq P_{\text{CHP}}^{\max} \tag{6}$$

The generated thermal energy can be directly supplied to heating loads or further utilized by absorption chillers to provide cooling energy.

F. ENERGY BALANCE CONSTRAINTS

To maintain reliable operation, the integrated energy system must satisfy electricity, heating, and cooling balance constraints at each scheduling period. These balance equations ensure coordinated multi-energy operation and are consistent with energy hub-based integrated energy modeling methods [1,3,12]. The electrical energy balance is expressed as:

$$P_{\text{PV}}(t) + P_{\text{CHP}}(t) + P_{\text{grid}}(t) + P_{\text{dis}}(t) = P_{\text{load}}(t) + P_{\text{ch}}(t) \tag{7}$$

The thermal energy balance is given by:

$$Q_{\text{CHP}}(t) + Q_{\text{boiler}}(t) = Q_{\text{heat}}(t) \tag{8}$$

The cooling energy balance is expressed as:

$$Q_{\text{chiller}}(t) + Q_{\text{abs}}(t) = Q_{\text{load,cool}}(t) \tag{9}$$

where $Q_{\text{chiller}}(t)$ denotes the cooling output of the electric chiller and $Q_{\text{abs}}(t)$ represents the cooling energy generated by the absorption chiller. This equation ensures the equality logic between the total supply from various cooling equipment and the actual cooling demand $Q_{\text{load,cool}}(t)$.

G. CARBON EMISSION MODELING

To evaluate environmental performance, carbon emissions associated with grid electricity consumption and natural gas utilization are incorporated into the operational optimization framework [11,14]. Total carbon emissions are calculated as:

$$E_{\text{CO2}} = \sum_{t=1}^{T} \left[\alpha_{\text{grid}} P_{\text{grid}}(t) + \alpha_{\text{gas}} F_{\text{gas}}(t)\right] \Delta t \tag{10}$$

where α_{grid} is the emission factor of grid electricity, and α_{gas} is the emission factor of natural gas. The carbon emission model is integrated into the multi-objective optimization framework to support low-carbon operational scheduling of the HSA integrated energy system.

III. MULTI-OBJECTIVE OPTIMIZATION METHOD

A. OPTIMIZATION OBJECTIVES

To improve the operational performance of the highway service area integrated energy system (HSA-IES), a multi-objective optimization framework is established by simultaneously considering economic efficiency, environmental impact, and renewable energy utilization. Since these objectives are inherently conflicting, Pareto-based multi-objective optimization is adopted to balance different operational requirements [5-7]. For example, reducing grid electricity purchase may lower operational cost during valley-price periods but increase the operating frequency of CHP units and associated carbon emissions. Similarly, maximizing renewable energy utilization may require more frequent ESS charging and discharging operations, thereby affecting operational cost and equipment degradation.

The first objective is to minimize the total operational cost of the system, including grid electricity purchase cost, natural gas consumption cost, equipment operation and maintenance cost, and EV charging operation cost [11-14]. The economic objective function is expressed as:

$$\begin{aligned} F_1 = \min \sum_{t=1}^{T} \big[& C_{\text{grid}}(t) P_{\text{grid}}(t) + C_{\text{gas}} F_{\text{gas}}(t) \\ & + C_{\text{om}}(t) + C_{\text{EV}}(t) \big] \end{aligned} \tag{11}$$

where $C_{\text{grid}}(t)$ denotes the electricity price at time t, C_{gas} is the natural gas price, $C_{\text{om}}(t)$ represents equipment operation and maintenance cost, and $C_{\text{EV}}(t)$ denotes EV charging operation cost.

The second objective is to minimize carbon dioxide emissions generated during system operation. Carbon emissions from both grid electricity consumption and natural gas utilization are considered:

$$F_2 = \min \sum_{t=1}^{T} \left[\alpha_{\text{grid}} P_{\text{grid}}(t) + \alpha_{\text{gas}} F_{\text{gas}}(t)\right] \Delta t \tag{12}$$

where α_{grid} is the carbon emission factor of grid electricity, and α_{gas} denotes the carbon emission factor of natural gas.

The third objective is to maximize renewable energy utilization efficiency while reducing renewable energy curtailment [8,15]. To unify the optimization direction of all objectives, the renewable energy utilization objective is transformed into a minimization form:

$$F_3 = \min \left(1 - \frac{\sum_{t=1}^{T} P_{\text{PV,used}}(t)}{\sum_{t=1}^{T} P_{\text{PV,total}}(t)}\right) \tag{13}$$

where $P_{\text{PV,used}}(t)$ represents the utilized photovoltaic power, and $P_{\text{PV,total}}(t)$ denotes the total available photovoltaic generation.

Through simultaneous optimization of the above objectives, the proposed framework aims to achieve balanced economic, environmental, and operational performance for highway service area energy systems.

B. DECISION VARIABLES

The operational optimization process involves multiple controllable variables associated with energy generation, storage, and flexible load scheduling. The main decision variables are summarized in Table 1.

The EV charging scheduling variable is introduced to improve load flexibility during peak traffic periods. By adjusting charging demand within allowable scheduling intervals, the operational pressure of the HSA inte grated energy system can be effectively reduced. Real-number encoding is adopted to represent continuous operational scheduling variables in the NSGA-II optimization process.

C. NSGA-II-BASED MULTI-OBJECTIVE OPTIMIZATION ALGORITHM

To solve the proposed multi-objective optimization problem, an enhanced version of the Non-dominated Sorting Genetic Algorithm II (NSGA-II) is employed. The theoretical improvement involves a specialized crowding-distance calculation that prioritizes solutions with higher resilience to load spikes, specifically tailored for the transient energy peaks in highway infrastructures [5-7]. Compared with conventional optimization methods such as particle swarm optimization (PSO), NSGA-II demonstrates better Pareto-front diversity and stronger adaptability in complex multi-energy scheduling problems.

The optimization procedure mainly consists of the following steps: Initialize the population and generate feasible operational scheduling strategies; Evaluate objective functions and calculate fitness values; Perform non-dominated sorting and crowding-distance calculation; Conduct selection, crossover, and mutation operations; Generate offspring populations; Update the population by combining parent and offspring populations; Check convergence conditions and terminate the optimization process when the maximum iteration number is reached or when the Pareto-front variation falls below the predefined threshold; Output the final Pareto front; Select the compromise solution using the minimum normalized distance method.

Figure 2 illustrates the overall optimization procedure of the proposed HSA integrated energy management framework. To improve optimization robustness, renewable energy fluctuations and load uncertainties are incorporated into the optimization process using band-limited stochastic disturbance signals with uniformly distributed amplitudes. Multiple repeated optimization runs are conducted to reduce the influence of random disturbances on the final results.

D. CONSTRAINT CONDITIONS

The optimization process must satisfy multiple operational constraints to ensure secure, stable, and economically feasible operation of the HSA integrated energy system.

1) Electricity Balance Constraint

The electricity balance constraint ensures real-time power equilibrium between generation and demand [1,3,12], as shown in Eq. (14):

$$P_{\mathrm{PV}}(t) + P_{\mathrm{CHP}}(t) + P_{\mathrm{grid}}(t) + P_{\mathrm{dis}}(t) = P_{\mathrm{load}}(t) + P_{\mathrm{ch}}(t) \tag{14}$$

where $P_{\mathrm{PV}}(t)$ is photovoltaic output power, $P_{\mathrm{CHP}}(t)$ is CHP electrical output, and $P_{\mathrm{grid}}(t)$ denotes purchased grid electricity.

2) Thermal and Cooling Balance Constraints

The thermal energy balance constraint is expressed as:

$$Q_{\mathrm{CHP}}(t) + Q_{\mathrm{boiler}}(t) = Q_{\mathrm{heat}}(t) \tag{15}$$

The cooling energy balance is expressed as:

$$Q_{\mathrm{cool}}(t) = Q_{\mathrm{load,cool}}(t) \tag{16}$$

These constraints ensure sufficient heating and cooling energy supply during all scheduling periods.

3) Energy Storage Constraints

The state of charge (SOC) of the ESS must remain within allowable operational limits:

$$SOC_{\min} \le SOC(t) \le SOC_{\max} \tag{17}$$

Charging and discharging power are constrained by:

$$0 \le P_{\mathrm{ch}}(t) \le P_{\mathrm{ch}}^{\max} \quad (18$$

$$0 \le P_{\mathrm{dis}}(t) \le P_{\mathrm{dis}}^{\max} \tag{19}$$

Simultaneous charging and discharging operations are prohibited during each scheduling interval to avoid unrealistic ESS operation.

4) CHP Operational Constraints

The CHP unit output is constrained by minimum and maximum operating limits [8,10]:

$$P_{\mathrm{CHP}}^{\min} \le P_{\mathrm{CHP}}(t) \le P_{\mathrm{CHP}}^{\max} \quad (20$$

To reflect realistic operational dynamics, CHP ramp-rate constraints are also considered:

$$|P_{\mathrm{CHP}}(t) - P_{\mathrm{CHP}}(t-1)| \le R_{\mathrm{CHP}} \tag{21}$$

where R_{CHP} denotes the maximum ramping capability of the CHP unit.

TABLE 1. Main Decision Variables of the HSA-IES Optimization Model

Variable Type	Symbol	Description
Grid electricity purchase power	$P_{\mathrm{grid}}(t)$ (14)	Power purchased from the grid
CHP output power	$P_{\mathrm{CHP}}(t)$ (15)	Electrical output of the CHP unit
ESS charging power	$P_{\mathrm{ch}}(t)$ (16)	Charging power of the ESS
ESS discharging power	$P_{\mathrm{dis}}(t)$ (17)	Discharging power of the ESS
Boiler thermal output	$Q_{\mathrm{boiler}}(t)$ (18)	Thermal output of the boiler
Chiller cooling output	$Q_{\mathrm{cool}}(t)$ (19)	Cooling output of the electric chiller
Renewable energy utilization	$P_{\mathrm{PV,used}}(t)$ (20)	Utilized photovoltaic power
Flexible EV charging scheduling	$P_{\mathrm{EV,shift}}(t)$ (21)	Shifted EV charging demand

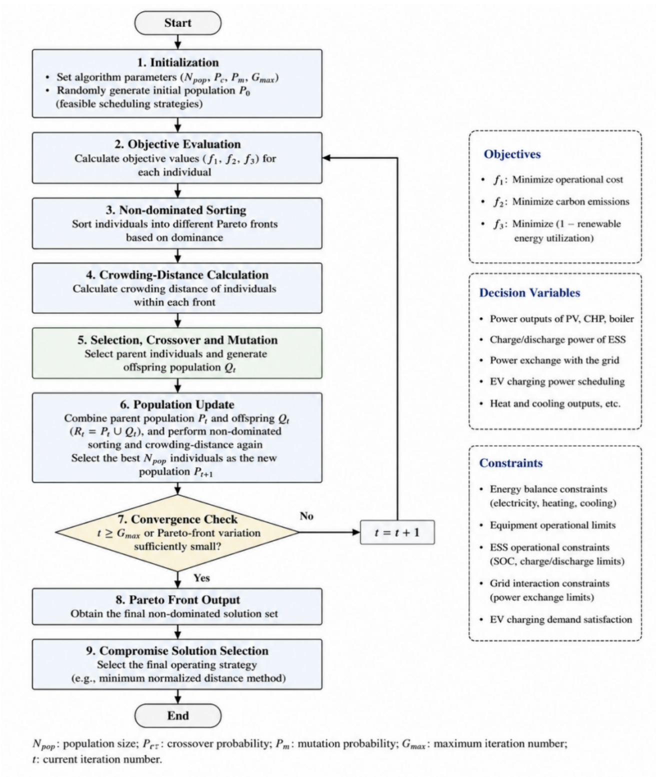

FIGURE 2. Overall optimization procedure of the proposed HSA integrated energy management framework

5) Renewable Energy Utilization Constraint

To avoid unrealistic renewable energy dispatch results, photovoltaic power utilization is constrained as:

$$0 \leq P_{\mathrm{PV,used}}(t) \leq P_{\mathrm{PV,total}}(t) \tag{22}$$

This constraint ensures that renewable energy utilization remains within physically available generation limits.

6) Grid Interaction Constraint

Grid electricity purchase is constrained by transmission capacity limitations:

$$0 \leq P_{\mathrm{grid}}(t) \leq P_{\mathrm{grid}}^{\mathrm{max}} \tag{23}$$

This constraint prevents excessive dependence on external grid supply and improves system operational security.

E. PARETO SOLUTION SELECTION STRATEGY

The proposed NSGA-II algorithm generates a set of Pareto-optimal operational solutions representing different trade-offs among operational cost, carbon emissions, and renewable energy utilization. To determine a practical compromise solution for system operation, the minimum normalized distance method is adopted to select the final operational strategy from the Pareto front.

The compromise solution is selected according to the minimum Euclidean distance between each Pareto solution and the ideal optimization point in the normalized objective space. This approach enables balanced consideration of economic performance, environmental impact, and renewable energy utilization. The selected compromise solution is subsequently used for simulation analysis and operational performance evaluation in the following section.

IV. CASE STUDY AND SIMULATION ANALYSIS

A. CASE DESCRIPTION

To verify the effectiveness of the proposed multi-objective optimization strategy, a typical medium-sized highway service area (HSA) integrated energy system located in eastern China is selected as the simulation case. The service area mainly includes commercial facilities, lighting systems, ventilation equipment, restaurants, heating and cooling systems, and electric vehicle (EV) charging stations. The integrated energy system consists of photovoltaic (PV) generation units, combined heat and power (CHP) units, battery energy storage systems (ESSs), gas boilers, electric chillers, and grid interaction modules.

The simulation is conducted over a 24 h scheduling horizon with a time interval of 1 h. Typical daily load profiles are established according to highway traffic flow characteristics and practical service-area energy consumption patterns. The electrical load profile exhibits two major peak periods at approximately 10:00– 12:00 and 18:00–21:00, mainly due to increased traffic flow and EV charging demand. PV output reaches its maximum around midday under typical solar irradiance conditions.

The peak electrical load of the HSA reaches approximately 920 $\pm$ 35 kW during evening charging periods, while the average daily electricity consumption is approximately 11.4 $\pm$ 0.5 MWh. EV charging demand accounts for approximately 20%–30% of the total electrical load during peak traffic periods. In addition, the average daily PV generation is approximately 2.1 $\pm$ 0.2 MWh under normal weather conditions. The equipment capacities are selected according to the typical energy demand scale of medium-sized highway service areas and practical integrated energy system configurations reported in previous studies [11-16]. The main equipment parameters of the proposed HSA-IES are summarized in Table 2.

TABLE 2. Main Parameters of the HSA Integrated Energy System

Component	Parameter	Value
PV system	Installed capacity	550 kW
ESS	Maximum capacity	900 kWh
ESS	Maximum charging/discharging power	250 kW
CHP unit	Rated electrical power	450 kW
CHP unit	Electrical efficiency	0.36
CHP unit	Thermal efficiency	0.44
Gas boiler	Rated thermal power	320 kW
Electric chiller	Rated cooling power	280 kW
Grid interaction	Maximum purchase power	1200 kW

The electricity price follows a time-of-use pricing mechanism. The peak-period electricity price is 1.12 RMB/kWh, while the flat-period and valley-period electricity prices are 0.76 RMB/kWh and 0.42 RMB/kWh, respectively. The natural gas price is assumed to be 3.2 RMB/m^3 according to local commercial energy tariffs.

B. SIMULATION PARAMETER SETTINGS

The proposed multi-objective optimization framework is implemented in MATLAB R2023a using the Non-dominated Sorting Genetic Algorithm II (NSGA-II) [5]. The main optimization parameters are listed in Table 3.

TABLE 3. NSGA-II Parameter Settings

Parameter	Value
Population size	120
Maximum iteration number	250
Crossover probability	0.90
Mutation probability	0.08
Pareto archive size	120

To improve result reliability and reduce the influence of stochastic disturbances, each simulation scenario is repeated five times under different random fluctuation conditions. Repeated simulations are conducted to reduce the influence of renewable energy intermittency and random load disturbances on optimization results.

The PV output is modeled with stochastic irradiance fluctuations of approximately $\pm$15%, while electrical load demand varies within $\pm$10%–25% to maintain consistency with the load modeling assumptions and to simulate high-traffic scenarios typical of holiday travel. To evaluate system robustness under extreme operating conditions, renewable energy uncertainty is increased to $\pm$20% in the high-fluctuation scenario. To avoid unrealistic idealized disturbances, renewable energy and load fluctuations are generated using band-limited stochastic disturbances rather than ideal Gaussian white noise. This approach better reflects practical operational characteristics of highway service area integrated energy systems.

C. SIMULATION SCENARIOS

To comprehensively evaluate the operational performance of the proposed strategy, three representative simulation scenarios are designed.

1) Scenario 1: Conventional Rule-Based Operation

In this scenario, the HSA integrated energy system operates using a conventional rule-based scheduling strategy without multi-objective optimization. The system mainly relies on grid electricity purchase and fixed CHP operating strategies. Renewable energy utilization and ESS coordination are not fully optimized. Therefore, this scenario is used as the baseline case for comparison.

2) Scenario 2: Multi-Objective Optimization Strategy

In this scenario, the proposed NSGA-II-based multi-objective optimization framework is applied. Operational cost, carbon emissions, and renewable energy utilization are simultaneously optimized under all operational constraints. Coordinated scheduling among PV generation, CHP units, ESSs, and grid interaction modules is fully considered.

3) Scenario 3: High Renewable and EV Charging Fluctuation Condition

To evaluate system robustness under more challenging operating conditions, significant renewable energy fluctuations and increased EV charging demand are introduced. PV output uncertainty is increased to approximately $\pm 20\%$, while EV charging demand increases by approximately 35% compared with normal operating conditions. This scenario is designed to represent holiday traffic peaks and adverse weather conditions.

D. EVALUATION INDICATORS

Several evaluation indicators are adopted to quantitatively assess the operational performance of the proposed HSA integrated energy system.

1) Economic Indicator

The total operational cost is used to evaluate system economic performance:

$$C_{\text{total}} = \sum_{t=1}^{T} \left(C_{\text{grid}}(t) + C_{\text{gas}}(t) + C_{\text{om}}(t) \right) \tag{24}$$

where: $C_{\text{grid}}(t)$ is grid electricity purchase cost, $C_{\text{gas}}(t)$ is natural gas consumption cost, $C_{\text{om}}(t)$ denotes equipment operation and maintenance cost.

2) Environmental Indicator

Carbon dioxide emissions are adopted to evaluate environmental performance:

$$E_{\text{CO2}} = \sum_{t=1}^{T} \left(\alpha_{\text{grid}} P_{\text{grid}}(t) + \alpha_{\text{gas}} F_{\text{gas}}(t) \right) \Delta t \tag{25}$$

Lower carbon emissions indicate better environmental benefits and higher renewable energy accommodation capability.

3) Renewable Energy Utilization Ratio

Renewable energy utilization efficiency is calculated as:

$$R_{\text{RES}} = \frac{\sum_{t=1}^{T} P_{\text{PV}}^{\text{used}}(t)}{\sum_{t=1}^{T} P_{\text{PV}}^{\text{total}}(t)} \tag{26}$$

This indicator reflects the renewable energy accommodation capability of the integrated energy system.

4) Operational Robustness Indicator

To evaluate system robustness under stochastic operating conditions, the standard deviations of operational cost and renewable energy utilization are calculated based on repeated simulation runs. Lower standard deviation values indicate stronger operational robustness and better adaptability to renewable energy fluctuations and load uncertainties.

E. SIMULATION ENVIRONMENT

All simulations were performed in MATLAB R2023a on a workstation equipped with an Intel Core i7 processor and 32 GB RAM. The optimization process adopted an hourly scheduling interval and incorporated stochastic renewable energy disturbances to improve simulation realism.

The simulation framework included load profile modeling, photovoltaic generation modeling, multi-objective optimization scheduling, and operational performance evaluation. Figure 3 shows the typical daily profiles of electrical load, EV charging demand, and PV generation used in the simulation.

V. RESULTS

A. PARETO OPTIMIZATION RESULTS

The proposed NSGA-II-based multi-objective optimization framework was applied to the highway service area integrated energy system (HSA-IES) under the simulation scenarios described in Section 4. Figure 4 presents the Pareto-optimal solution distribution obtained during the optimization process. Clear trade-off relationships among operational cost, carbon emissions, and renewable energy utilization can be observed.

As shown in Figure 4, solutions with lower operational cost generally rely more heavily on grid electricity purchase and conventional energy supply, whereas solutions with lower carbon emissions require higher renewable energy accommodation and more frequent ESS operation. In addition, excessive pursuit of renewable energy utilization may increase ESS cycling frequency and the operational adjustment complexity of CHP units. Therefore, no single solution can simultaneously optimize all objectives, which demonstrates the necessity of Pareto-based multi-objective optimization.

To obtain a practical operational strategy, the compromise solution with the minimum normalized Euclidean distance from the ideal optimization point is selected from the Pareto front. This solution provides a balanced trade-off among economic efficiency, environmental impact, and renewable energy utilization.

B. OPERATIONAL PERFORMANCE COMPARISON

Table 4 summarizes the operational performance comparison between the conventional rule-based strategy and the proposed optimization strategy under normal operating conditions. The reported values are expressed as the mean $\pm$ standard deviation of five repeated simulations under stochastic renewable generation and load fluctuations.

Compared with the conventional strategy, the proposed optimization method reduces the total operational cost by approximately 12.7%. Carbon emissions decrease by approximately 18.2%, while renewable energy utilization increases from 72.6% to 86.1%. The improvement in renewable energy utilization is more pronounced than the cost reduction because part of the economic benefit is offset by increased ESS cycling and CHP adjustment costs.

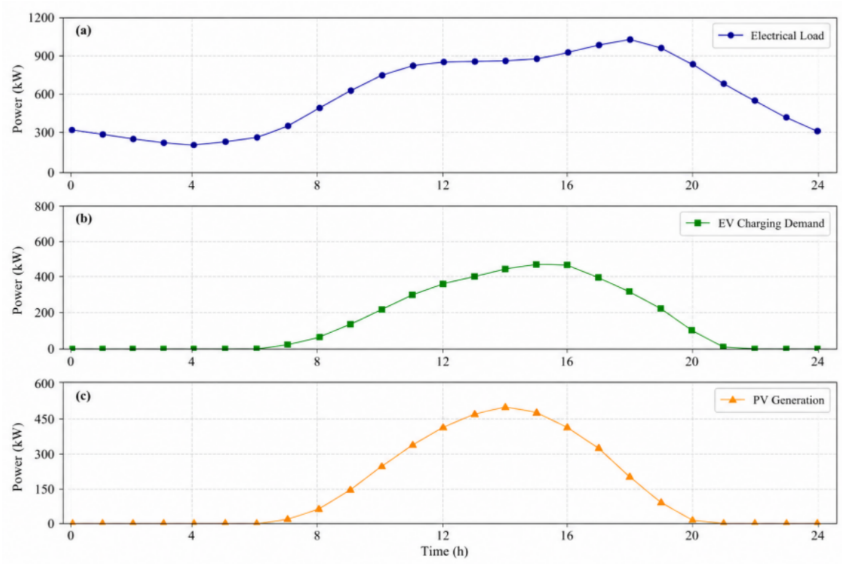

FIGURE 3. Typical daily profiles of electrical load, EV charging demand, and PV generation

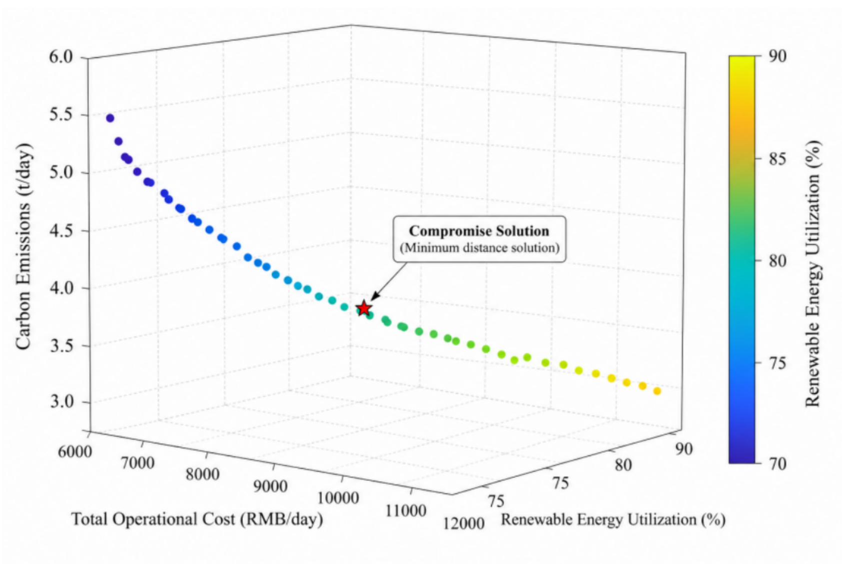

FIGURE 4. Pareto front distribution considering operational cost, carbon emissions, and renewable energy utilization

TABLE 4. Operational Performance Comparison Under Normal Conditions

Indicator	Conventional Strategy	Proposed Strategy
Total operational cost (RMB/day)	8426 ± 218 (35)	7356 ± 227 (36)
Carbon emissions (t/day)	5.21 ± 0.17 (37)	4.26 ± 0.18 (38)
Renewable energy utilization ratio (%)	72.6 ± 2.4 (39)	86.1 ± 2.3 (40)
Grid electricity purchase (MWh/day)	8.42 ± 0.31 (41)	6.92 ± 0.33 (42)

The observed standard deviations are mainly caused by stochastic renewable generation fluctuations and random EV charging demand variations.

The reduction in grid electricity purchase mainly results from coordinated scheduling among photovoltaic generation, CHP operation, and ESS charging/discharging strategies. During daytime periods with strong solar irradiance, surplus photovoltaic power is preferentially stored in the ESS for later use during peak-demand periods. Meanwhile, flexible EV charging scheduling shifts part of the charging demand from peak-price periods to flat-price periods, thereby reducing peak grid electricity purchase.

Compared with previous integrated energy scheduling studies [11-16], the proposed strategy achieves comparable carbon reduction performance while maintaining stable renewable energy accommodation capability under highly dynamic EV charging conditions.

C. ENERGY SCHEDULING ANALYSIS

Figure 5 illustrates the optimized operational scheduling results for a typical operating day. As shown in Figure 5(a), photovoltaic output increases significantly after 08:00 and reaches its maximum around midday, supplying a substantial proportion of the electrical load. During this period, surplus PV power is preferentially stored in the ESS to improve renewable energy accommodation efficiency.

Figure 5(b) shows the ESS charging and discharging profiles under the optimized strategy. The ESS mainly charges during daytime PV peak periods and discharges during evening peak-load periods between 18:00 and

21:00, effectively reducing grid electricity purchase and alleviating peak-load pressure. Figure 5(c) presents the grid power exchange profile under the optimized scheduling strategy. During periods of high photovoltaic generation, grid electricity purchase decreases significantly, and partial surplus renewable energy can be utilized to reduce external power dependence. In contrast, grid electricity purchase increases during nighttime and late-evening periods when renewable energy generation is insufficient. Figure 5(d) illustrates the coordinated operational relationship between CHP electrical output and thermal demand. The CHP unit mainly operates during medium and high thermal demand periods, simultaneously providing electricity and thermal energy. Compared with the conventional scheduling strategy, the optimized strategy reduces unnecessary CHP output fluctuations, thereby improving operational stability and reducing natural gas consumption.

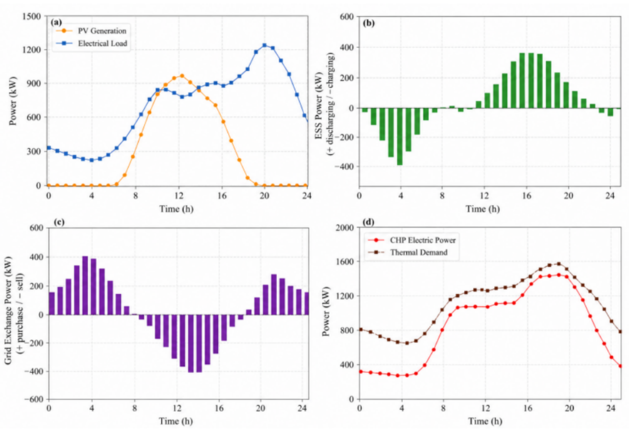

FIGURE 5. Optimized operational scheduling results for a typical operating day

No infeasible operational conditions or energy supply shortages are observed during repeated stochastic simulations, indicating that the proposed optimization framework has good operational robustness.

D. PERFORMANCE UNDER HIGH-FLUCTUATION CONDITIONS

To further evaluate system robustness, the proposed strategy is tested under high renewable energy fluctuation and increased EV charging demand conditions. In this scenario, renewable generation uncertainty is increased to $\pm 20\%$, while EV charging demand increases by approximately 35% compared with normal operating conditions.

Table 5 summarizes the operational performance under the high-fluctuation scenario.

TABLE 5. Operational Performance Under High-Fluctuation Conditions

Indicator	Conventional Strategy	Proposed Strategy
Total operational cost (RMB/day)	9175 ± 286 (43)	7814 ± 241 (44)
Carbon emissions (t/day)	5.86 ± 0.23 (45)	4.63 ± 0.19 (46)
Renewable energy utilization ratio (%)	68.1 ± 3.1 (47)	82.9 ± 2.6 (48)
Grid electricity purchase (MWh/day)	9.26 ± 0.35 (49)	7.48 ± 0.31 (50)

Although renewable energy uncertainty and EV charging demand increase significantly under this scenario, the proposed optimization framework maintains relatively stable operational performance. The standard deviation of operational cost increases moderately due to intensified renewable energy fluctuations, but the proposed optimization strategy still outperforms the conventional scheduling method under all tested indicators.

Compared with the conventional strategy, the proposed method achieves approximately 14.8% operational cost reduction and approximately 21.0% carbon emission reduction under high-fluctuation conditions. In addition, renewable energy utilization improves from 68.1% to 82.9%, indicating that the proposed strategy can effectively enhance renewable energy accommodation even under intensified uncertainty. These results demonstrate the strong adaptability of the proposed optimization strategy under high renewable penetration and fluctuating EV charging demand.

E. SENSITIVITY ANALYSIS OF ESS CAPACITY

To investigate the influence of ESS capacity on system performance, the ESS capacity is varied from 400 kWh to 1200 kWh. Figure 6 illustrates the relationship between ESS capacity and key operational indicators. As ESS capacity increases, renewable energy utilization gradually improves due to the enhanced energy-shifting capability of the storage system, while grid electricity purchase during peak-price periods decreases. However, when the ESS capacity exceeds approximately 1000 kWh, the reduction in operational cost becomes relatively limited because most surplus daytime PV energy has already been effectively accommodated. In terms of economic feasibility, while increasing capacity optimizes operational costs (OPEX), it concurrently leads to a substantial rise in initial capital expenditure (CAPEX). Therefore, the total lifecycle cost (including both investment and operation) must be carefully weighed. Excessively large ESS capacity will diminish the marginal economic returns, as the high investment costs of additional storage units often outweigh the savings generated from further grid power reduction. Consequently, an optimized capacity range is essential for HSA managers to ensure a balance between environmental targets and long-term financial viability.

VI. DISCUSSION

The simulation results demonstrate that the proposed NSGA-II-based multi-objective optimization framework can effectively improve the economic and environmental performance of highway service area integrated energy systems. Coordinated scheduling among photovoltaic generation, CHP units, ESSs, and flexible EV charging demand significantly enhances renewable energy accommodation capability while reducing operational cost and carbon emissions.

The proposed framework also exhibits good adaptability under stochastic renewable energy fluctuations and increased EV charging demand conditions. This characteristic is particularly important for highway service areas, where traffic flow and charging demand may vary significantly over time.

However, several limitations still exist in the current study. First, the proposed model mainly focuses on day-ahead operational scheduling and does not consider detailed real-time control dynamics or electricity market interactions. Second, EV charging demand is modeled using aggregated load characteristics rather than detailed user charging behavior. Third, battery degradation cost and long-term lifecycle effects of the ESS are not explicitly considered. Frequent charging and discharging operations may influence battery lifetime and additional maintenance cost under practical operating conditions. Future work will further investigate multiservice-area coordinated scheduling, real-time predictive control, integrated electricity market participation, and battery degradation modeling.

VII. CONCLUSION

This study proposed a multi-objective optimization framework for the operational scheduling of highway service area integrated energy systems (HSA-IESs). The proposed framework integrates photovoltaic generation, combined heat and power (CHP) units, battery energy storage systems (ESSs), flexible electric vehicle (EV) charging demand, and grid interaction modules within a unified coordinated energy management model. The Non-dominated Sorting Genetic Algorithm II (NSGA-II) was employed to simultaneously optimize operational cost, carbon emissions, and renewable energy utilization under stochastic renewable generation and load fluctuation conditions.

Simulation results demonstrate that the proposed optimization strategy effectively improves both economic and environmental performance compared with the conventional rule-based operational strategy. Under typical operating conditions, the proposed method reduces operational cost by approximately 12.7% and carbon emissions by approximately 18.2%, while renewable energy utilization increases by 13.5 percentage points. Coordinated scheduling among renewable generation, ESSs, CHP units, and flexible EV charging demand effectively reduces peak-period grid electricity purchase and improves overall renewable energy accommodation capability.

The proposed framework also maintains stable operational performance under high renewable energy fluctuation and increased EV charging demand conditions, demonstrating good scheduling adaptability and operational robustness. Compared with conventional scheduling methods, the proposed framework simultaneously considers renewable energy accommodation, flexible EV charging demand, and stochastic operational uncertainty within a unified multi-objective optimization structure. Therefore, the proposed strategy is particularly suitable for highway service areas characterized by highly dynamic traffic flow and EV charging demand. Overall, the proposed optimization framework can provide practical decision support for low-carbon and intelligent energy management of future highway transportation infrastructures with high renewable energy penetration. However, the current study mainly focuses on day-ahead operational scheduling and does not consider detailed real-time control dynamics, battery degradation effects, or electricity market participation mechanisms. Future work will further investigate real-time traffic-flow prediction, vehicle-to-grid interaction, dynamic electricity pricing, battery degradation modeling, and coordinated scheduling among multiple highway service areas to further enhance system operational flexibility and economic performance.

AUTHOR CONTRIBUTIONS

Conceptualization – Yongjun Zhou, Menghao Duan, Junzu Liu, and Haipin Huang; methodology – Yongjun Zhou, Menghao Duan, Junzu Liu, and Haipin Huang; investigation – Yongjun Zhou, Menghao Duan, Junzu Liu, and Haipin Huang; writing–original draft preparation – Yongjun Zhou, Menghao Duan, Junzu Liu, and Haipin Huang. All authors have read and agreed to the published version of the manuscript.

CONFLICTS OF INTEREST

The authors declare no conflict of interest.

FUNDING

This research received no external funding.

ACKNOWLEDGEMENTS

Not applicable.

REFERENCES

[1] M. Geidl and G. Andersson, “Optimal power flow of multiple energy carriers,” IEEE Transactions on Power Systems, vol. 22, no. 1, pp. 145-155, 2007, doi: 10.1109/TPWRS.2006.888988.

[2] P. Mancarella, “MES (multi-energy systems): An overview of concepts and evaluation models,” Energy, vol. 65, pp. 1-17, 2014, doi: 10.1016/j.energy.2013.10.041.

[3] M. Mohammadi, Y. Noorollahi, B. Mohammadi-Ivatloo, and H. Yousefi, "Energy hub: From a model to a concept-A review," Renewable and Sustainable Energy Reviews, vol. 80, pp. 1512-1527, 2017, doi: 10.1016/j.rser.2017.07.030.

[4] J. Kennedy and R. Eberhart, "Particle swarm optimization," Proceedings of IEEE International Conference on Neural Networks, pp. 1942-1948, 1995, doi: 10.1109/ICNN.1995.488968.

[5] K. Deb, A. Pratap, S. Agarwal, and T. Meyarivan, "A fast and elitist multiobjective genetic algorithm: NSGA-II," IEEE Transactions on Evolutionary Computation, vol. 6, no. 2, pp. 182-197, 2002, doi: 10.1109/4235.996017.

[6] A. Coello Coello C, "Evolutionary multi-objective optimization: A historical view of the field," IEEE Computational Intelligence Magazine, vol. 1, no. 1, pp. 28-36, 2006, doi: 10.1109/MCI.2006.1597059.

[7] Q. Zhang and H. Li, "MOEA/D: A multiobjective evolutionary algorithm based on decomposition," IEEE Transactions on Evolutionary Computation, vol. 11, no. 6, pp. 712-731, 2007, doi: 10.1109/TEVC.2007.892759.

[8] X. Chen, C. Kang, M. O'Malley, et al., "Increasing the flexibility of combined heat and power for wind power integration in China: Modeling and implications," IEEE Transactions on Power Systems, vol. 30, no. 4, pp. 1848-1857, 2015, doi: 10.1109/ TPWRS.2014.2356723.

[9] J. Wang, H. Zhong, Z. Ma, et al., "Review and prospect of integrated demand response in the multi-energy system," Applied Energy, vol. 202, pp. 772-782, 2017, doi: 10.1016/j.apenergy.2017.05.150.

[10] F. Fang, H. Wang Q, and Y. Shi, "A novel optimal operational strategy for the CCHP system based on two operating modes," IEEE Transactions on Power Systems, vol. 27, no. 2, pp. 1032-1041, 2012, doi: 10.1109/TPWRS.2011.2175490.

[11] Z. Xiong, D. Zhang, and Y. Wang, "Optimal operation of integrated energy systems considering energy trading and integrated demand response," Energy Reports, vol. 11, pp. 5310-5324, 2024, doi: 10.1016/j.egyr.2024.03.010.

[12] T. Ma, J. Wu, and L. Hao, "Energy flow modeling and optimal operation analysis of the micro energy grid based on energy hub," Energy Conversion and Management, vol. 133, pp. 292-306, 2017, doi: 10.1016/j.enconman.2016.12.011.

[13] X. Zhang, M. Shahidehpour, A. Alabdulwahab, and A. Abusorrah, "Optimal expansion planning of energy hub with multiple energy infrastructures," IEEE Transactions on Smart Grid, vol. 6, no. 5, pp. 2302-2311, 2015, doi: 10.1109/tsg.2015.2390640.

[14] G. Li, R. Zhang, T. Jiang, et al., "Security-constrained bi-level economic dispatch model for integrated natural gas and electricity systems considering wind power and power-to-gas process," Applied Energy, vol. 194, pp. 696-704, 2017, doi: 10.1016/j.apenergy.2016.07.077.

[15] Y. Zhang, N. Gatsis, and B. Giannakis G, "Robust energy management for microgrids with high-penetration renewables," IEEE Transactions on Sustainable Energy, vol. 4, no. 4, pp. 944-953, 2013, doi: 10.1109/TSTE.2013.2255135.

[16] B. Zhao, X. Zhang, P. Li, et al., "Optimal sizing, operating strategy and operational experience of a stand-alone microgrid on Dongfushan Island," Applied Energy, vol. 113, pp. 1656-1666, 2014, doi: 10.1016/j.apenergy.2013.09.015.

[17] C. Wang, X. Zhang, X. Lu, and et al.Interval design of expressway comprehensive energy system based on multi-objective optimization, "International Conference on Smart Transportation and City Engineering (STCE 2023), 2024:221,", doi: 10.1117/12.3024747.

[18] S. Bahramirad, W. Reder, and A. Khodaei, "Reliability-constrained optimal sizing of energy storage system in a microgrid," IEEE Transactions on Smart Grid, vol. 3, no. 4, pp. 2056-2062, 2012, doi: 10.1109/TSG.2012.2217991.